Lazareva, Olesya ; Pichler, Thomas

Naturally occurring arsenic in the Miocene Hawthorn Group, southwestern Florida: Potential implication for phosphate mining

Journal Article as: peer-reviewed accepted version (Postprint)

DOI of this document*(secondary publication): https://doi.org/10.26092/elib/3246

Publication date of this document: 02/12/2024

* for better findability or for reliable citation

Recommended Citation (primary publication/Version of Record) incl. DOI:

Olesya Lazareva, Thomas Pichler, Naturally occurring arsenic in the Miocene Hawthorn Group, southwestern Florida: Potential implication for phosphate mining, Applied Geochemistry, Volume 22, Issue 5, 2007, Pages 953-973, ISSN 0883-2927, https://doi.org/10.1016/j.apgeochem.2006.12.021.

Naturally occurring arsenic in the Miocene Hawthorn Group, southwestern Florida: Potential implication for phosphate mining

Olesya Lazareva, Thomas Pichler [*]

Department of Geology, University of South Florida, Tampa, FL, USA

---

[*] Corresponding author. Tel.: +1 813 974 0321; fax: +1 813 974 2654.
E-mail address: pichler@shell.cas.usf.edu (T. Pichler).

1. Introduction

Southwestern Florida hosts several large phosphate mines that exploit the Oligocene- to Miocene-aged Hawthorn Group sediments (Blakey, 1973). Currently, Florida supplies about one-quarter of the world's and three-quarters of the United States domestic phosphate needs (Hodges et al., 2001).

Arsenic concentrations of up to 54.1 mg/kg were recently reported for samples from the Oligocene-aged Suwannee Limestone in Florida (Price and Pichler, 2006). The Suwannee Limestone directly underlies the Hawthorn Group, which triggered this study. Because P and As are chemically closely related, they often co-occur in nature (Shields, 2002). In addition, the highly open crystal structure of carbonate fluorapatite (francolite) shows a tendency to accumulate such elements as As, Mo, Se, Y, Zn and the Rare Earth Elements (REE) during diagenesis (Shields, 2002). This may pose problems for phosphate mining, such as (1) high As values in the phosphate-bearing rock has a negative effect on ore processing (benefication) and the quality of the final product; and (2) mine-induced changes in ground water physico-chemical conditions may cause the release of As present in the subsurface,

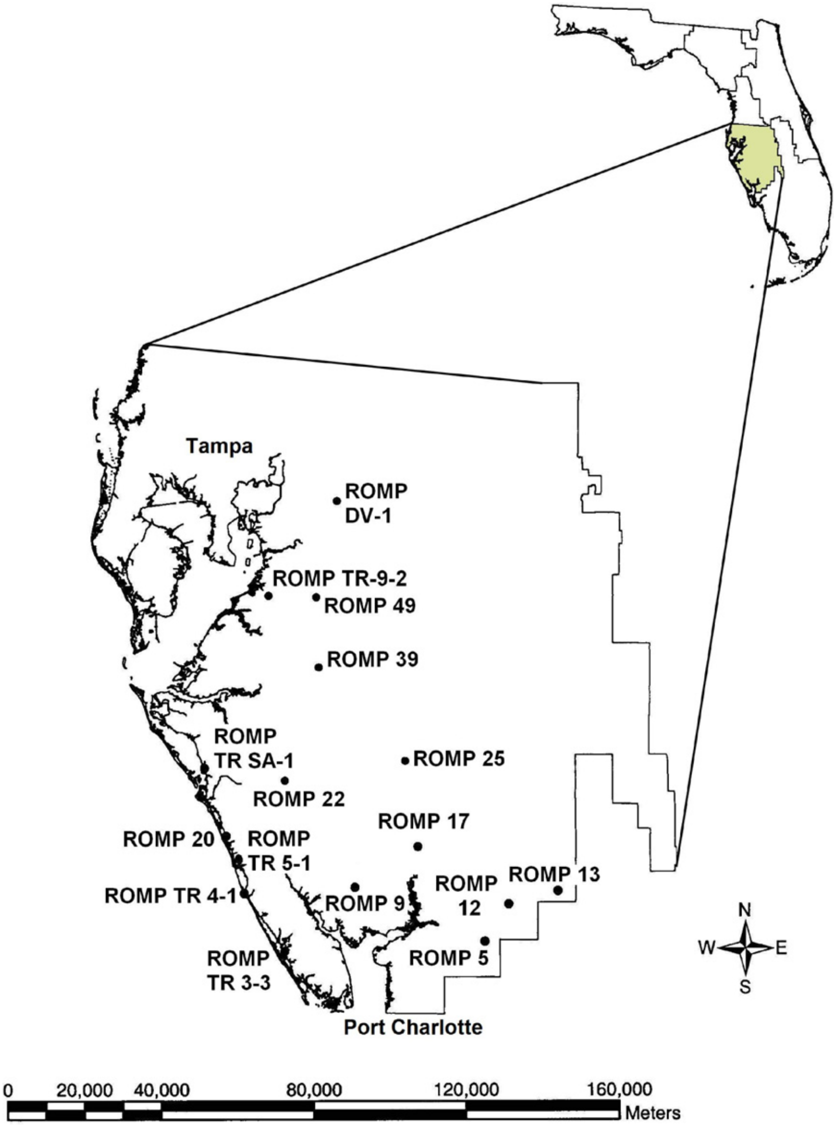

Fig. 1. Map of the research area including the Regional Observation Monitor Well Program (ROMP) locations, numbers, and names of the 16 cores that were sampled. Note: the sample labels correspond to drill 'well number' – 'sample depth'.

causing increased values in public and private supply wells relative to existing drinking water standards. The potential for this scenario was clearly demonstrated by release of high-As water from Coronet Industries processing plant in Plant City, Hillsborough County, where levels were in excess of 100 μg/L (Hammett, 2002). The new Maximum Contaminant Level (MCL) for As in drinking water, established by the U. S. Environmental Protection Agency (US EPA) in 2001 and which took effect on January 23, 2006, is 10 μg/L (Walsh, 2001). Moreover, there have been several occurrences of swine fatalities due to As contaminated phosphate feed supplements (El Bahri and Romdane, 1991).

1.1. Geology and hydrogeology of the study area

The research area is located in the Southwest Florida Water Management District (SWFWMD) between Tampa and Port Charlotte (Fig. 1). Here the hydrogeological framework can be subdivided into 3 discrete units, the Floridan Aquifer System (FAS), the Intermediate Aquifer System (IAS) or Intermediate Confining Unit, and the Surficial Aquifer System (SAS) (Fig. 2) (Miller, 1986).

The Miocene Hawthorn Group is the stratigraphic unit that contains the Intermediate aquifer system. It is subdivided into a lower section comprising the undifferentiated Arcadia Formation, Tampa and Nocatee Members of the Arcadia Formation (Fig. 2) and the upper section of the Peace River Formation (Scott, 1988, 1990). The Arcadia Formation unconformably overlies the Oligocene Suwannee Limestone. Its maximum thickness within the study area is approximately 183 m (600 ft) in the Okeechobee Basin (Scott, 1988). Throughout the research area the undifferentiated Arcadia Formation is principally composed of variable amount of siliciclastics

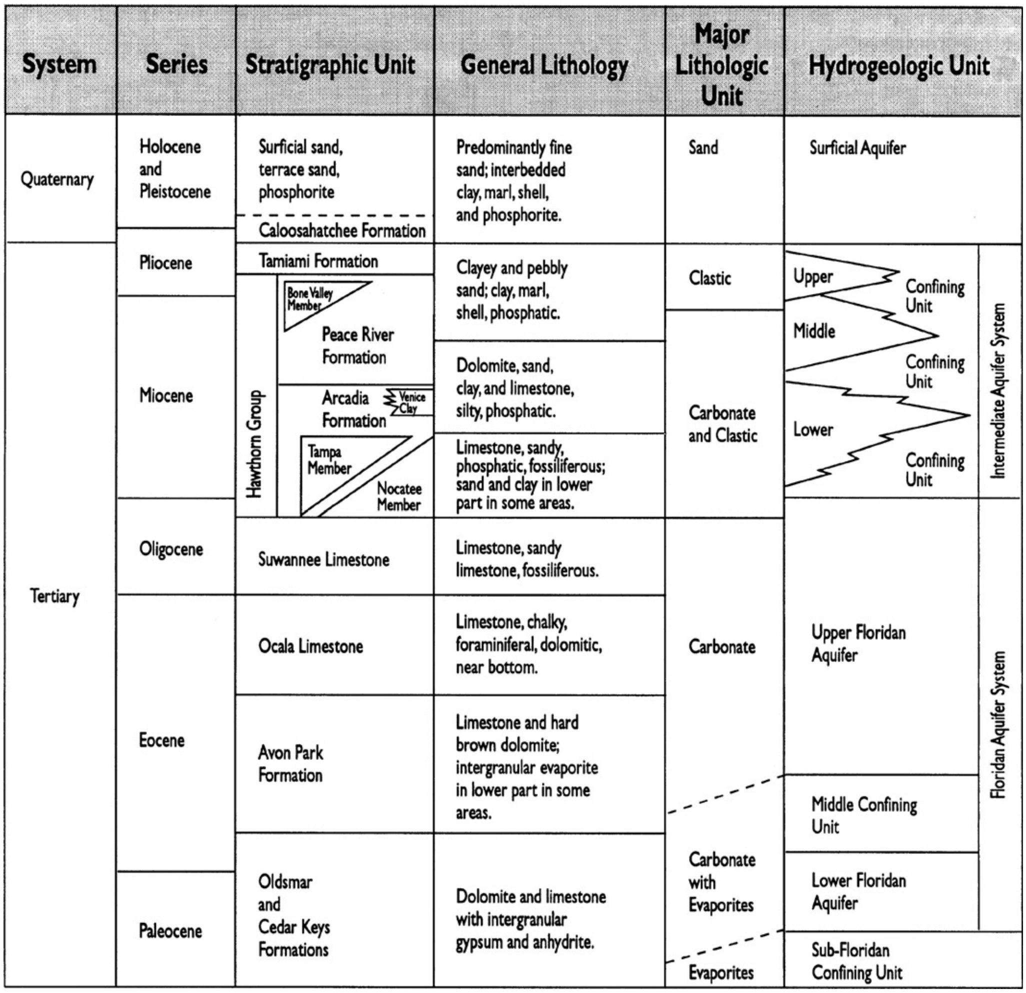

Fig. 2. Lithostratigraphic and hydrogeologic units of the study area (Modified from Miller, 1986).

such as quartz sands, greenish gray clays, chert and francolite within a carbonate matrix (Scott, 1990). The lithology of the Tampa Member of the Arcadia Formation varies from yellow-gray marine wackestone to packestone containing variable amounts of dolostone, clay, quartz sand and minor occurrences of francolite (Wingard et al., 1993; Scott, 1988). The Nocatee Member forms the base of the Arcadia Formation (Fig. 2) in the much of the southern portion of SWFWMD. Scott (1988) reported that the Nocatee Member contains the highest amount of siliciclastic material found within the entire Arcadia Formation.

The Peace River Formation, currently being exploited for the phosphate ore, unconformably overlies the Arcadia Formation (Fig. 2) and, within the study area, reaches a maximum thickness of 46–61 m (150–200 ft) in the Okeechobee Basin (Scott, 1990). In the study area, the Peace River Formation consists of greenish gray sandy clays, and carbonates with variable amounts of francolite, sand and gravel (Green et al., 1995). The carbonates are comprised of interbedded limestones, dolostones, and a siliciclastic component dominates the Peace River Formation (Scott, 1988).

2. Methods

A combination of petrographic and geochemical techniques was used to evaluate the abundance and mineralogical association of As in 362 samples from 16 Hawthorn Group cores in proximity to current and future phosphate mining. The cores were originally collected as part of the Regional Observation Monitor Well Program (ROMP) by SWFWMD, and stored at the Florida Geological Survey (FGS) in Tallahassee. Each core was sampled at an even spacing of approximately 7.5 m to ensure representation of the entire Hawthorn interval. In addition, targeted samples were taken from sections, which previous studies (Price and Pichler, 2006) suggested were likely to have higher As concentrations than the bulk carbonate/siliciclastic matrix, such as areas containing visible pyrite, hydrous ferric oxides, green clays, and organic material. Overall, 285 interval samples and 77 targeted samples were collected and analyzed. The sample labels correspond to drill 'well number' – 'sample depth' (for example, sample 12-48).

The samples were initially examined using a 10× hand lens and a stereo microscope. Based on a combination of hand specimen description and bulk As concentration (following chemical analyses), approximately 60 samples were selected for further study. Polished thin sections were made for those samples and they were examined using a polarizing microscope with reflected and transmitted light.

To determine bulk chemical composition samples were powdered (homogenized) in an agate mortar. To avoid cross-contamination, the mortar and pestle were cleaned with pure silica sand and deionised water between samples. A dilute HNO_3 solution was used after powdering soft greenish clays. Approximately 0.5 ± 0.001 g of powdered sample was weighed into a digestion vessel and 10 mL of a 3:1 mixture of HCl and HNO_3 was added. The digestion vessel was immediately capped with a reflux cup to trap any arsine gas. The sample was heated to a temperature of 95 °C for 30 min. After digestion, the solution was cooled, diluted to 50 mL (5:1) with DI water, centrifuged for 15 min to remove non-soluble particles, and filtered.

Calcium, Fe, Mg, Mn, S, P, Si and Al were determined on a Perkin Elmer Optima 2000 DV inductively coupled plasma – optical emission spectrometer (ICP-OES). Bulk As concentrations were measured by hydride generation-atomic fluorescence spectrometry using a PSA 10.055 Millenium Excalibur instrument (HG-AFS) at the Center for Water Analysis, University of South Florida. The accuracy and precision of the measurements and acid digestion was verified by analysis of the JGS JLs-1 reference material and sample duplicates, which indicated a precision of better than 5%. Reagent-acid blanks were tested and showed no detectable As. Background signal drift was consistently less than 1%.

Based on the bulk concentrations, samples with high As levels were selected for a more focused mineralogical analysis using a Hitachi S-3500N scanning electron microscope (SEM) at the College of Marine Science, University of South Florida.

To better understand the chemical composition of individual minerals and mineral phases containing As, 16 polished thin sections from each formation/member of the Hawthorn Group were chosen for electron-probe microanalysis – wave dispersive spectrometry (EMPA or electron microprobe), using a JEOL 8200 instrument at the University of New Mexico. Operating conditions of the electron microprobe were 20 kV accelerating voltage, a spot size of 5 μm, and a 20 nA current. The electron microprobe was used for spot analysis and to map As concentrations within the sample matrix and in individual minerals.

3. Results

3.1. Mineralogy and petrography

3.1.1. Arcadia Formation

Most samples consisted of carbonate material (limestones and dolostones), with a variable siliciclastic component, and francolite. The siliciclastics were primarily composed of gray and grayish green clays, and quartz. The Tampa Member contained minor or no francolite. The sedimentary components contained minor mineral phases, such as pyrite, gypsum, chert, secondary calcite, feldspar, and hydrous ferric oxides (HFOs). The HFOs were frequently observed as stains or rings around pyrites. Framboidal pyrite was ubiquitous throughout the Arcadia Formation. Organic matter was observed in several samples and revealed a heterogeneous distribution throughout the undifferentiated Arcadia Formation.

The examination of thin sections confirmed the presence of francolite, calcite, dolomite, feldspar, pyrite, quartz, clays, and HFO. Pyrite was present as framboids generally less 10 μm in diameter in about 90% of the thin sections, occurring in the sediment matrix and as inclusions in francolite nodules (Fig. 3). Framboids consisted of euhedral pyrite micro-crystals. These observations were confirmed by SEM (Fig. 4a).

3.1.2. Peace River Formation

The majority of samples from the Peace River sediments were composed of siliciclastics such as quartz sand, gray to dark greenish gray clays, and substantial amounts of francolite. Minor mineral phases were pyrite, gypsum, sulfur, secondary calcite, feldspar, and HFO. Most pyrite was present in the form of framboids; cubic pyrite (Fig. 4b) only occurred in one sample (12-125(2)).

Thin section examination confirmed the presence of pyrite, francolite, calcite, gypsum, dolomite, feldspar, quartz, clays and HFO. About 90% of the thin sections from the Peace River Formation contained pyrite crystals in the sediment matrix and several samples revealed pyrite inclusions in francolite grains and calcite crystals (Fig. 5).

3.2. Bulk rock chemical composition

Bulk As concentrations for all 362 Hawthorn Group samples varied from 0.1 to as high as 69.0 mg/kg with a mean (μ) of 5.6 mg/kg ($\sigma = 7.1$ mg/kg) (Table 1). Bulk-rock chemical analyses by ICP-OES for Ca, Mg, Mn, Fe, S, Al, P and Si showed that the strongest linear correlation for the Hawthorn Group sediments existed between S and Fe with a R^2 of 0.87 (Appendix 1), which could be due to the outlier effect (Swan and Sandilands, 1995) caused by sample 12-125(2) (Fig. 6a). This sample had anomalously high Fe, S and P compared to other Hawthorn Group sediments. Elimination of the outlier point changed the correlation coefficient to $R^2 = 0.77$ (Fig. 6b).

The total As concentrations of the 285 interval samples (samples that were taken at fixed intervals) ranged from 0.1 to 40.8 mg/kg with a mean of 5.0 mg/kg ($\sigma = 5.8$ mg/kg) (Table 1). Bulk-rock analyses by ICP-OES revealed a significant degree of linear correlation between Fe and S ($R^2 = 0.69$) for all interval samples (Fig. 7, Appendix 1).

The bulk As concentrations of the 77 targeted samples (samples likely to have high As concentrations) ranged from 0.4 to 69.0 mg/kg with a mean of 8.3 mg/kg ($\sigma = 10.5$ mg/kg) (Table 1). Bulk-rock analysis showed that a significant degree of linear correlation existed between Fe and S ($R^2 = 0.95$) for the all “special interest” samples (Appendix 1), which could be due to the outlier effect (Swan and Sandilands, 1995) caused by sample 12-125(2) (Fig. 8a). Elimination of the outlier point reduced the correlation coefficient to $R^2 = 0.83$ (Fig. 8b).

3.2.1. Arcadia Formation

The bulk As concentrations in samples from the undifferentiated Arcadia Formation varied from 0.1 to 36.0 mg/kg with a mean of 5.7 mg/kg ($\sigma = 6.2$ mg/kg) (Table 1). Approximately 88% and 11% of the samples had <10 mg/kg and <1 mg/kg As, respectively. Samples consisting mainly of limestone and dolostone showed low As concentrations, whereas higher concentrations were generally associated with pyrite, clay, HFO and francolite. A high degree of linear correlation for the undifferentiated Arcadia Formation sediments existed for S with Fe ($R^2 = 0.81$), and Al with Fe ($R^2 = 0.74$) (Appendix 1).

The bulk As concentrations in samples from the Tampa Member of the Arcadia Formation ranged from 0.2 to 15.2 mg/kg (Table 1). The mean value for 75 samples was 3 mg/kg ($\sigma = 3.7$ mg/kg). Approximately 92% and 39% of the samples contained <10 mg/kg and <1 mg/kg As, respectively. A high degree of linear correlation for the Tampa Member samples existed for Al with Fe ($R^2 = 0.76$), and Al with S ($R^2 = 0.78$). The most

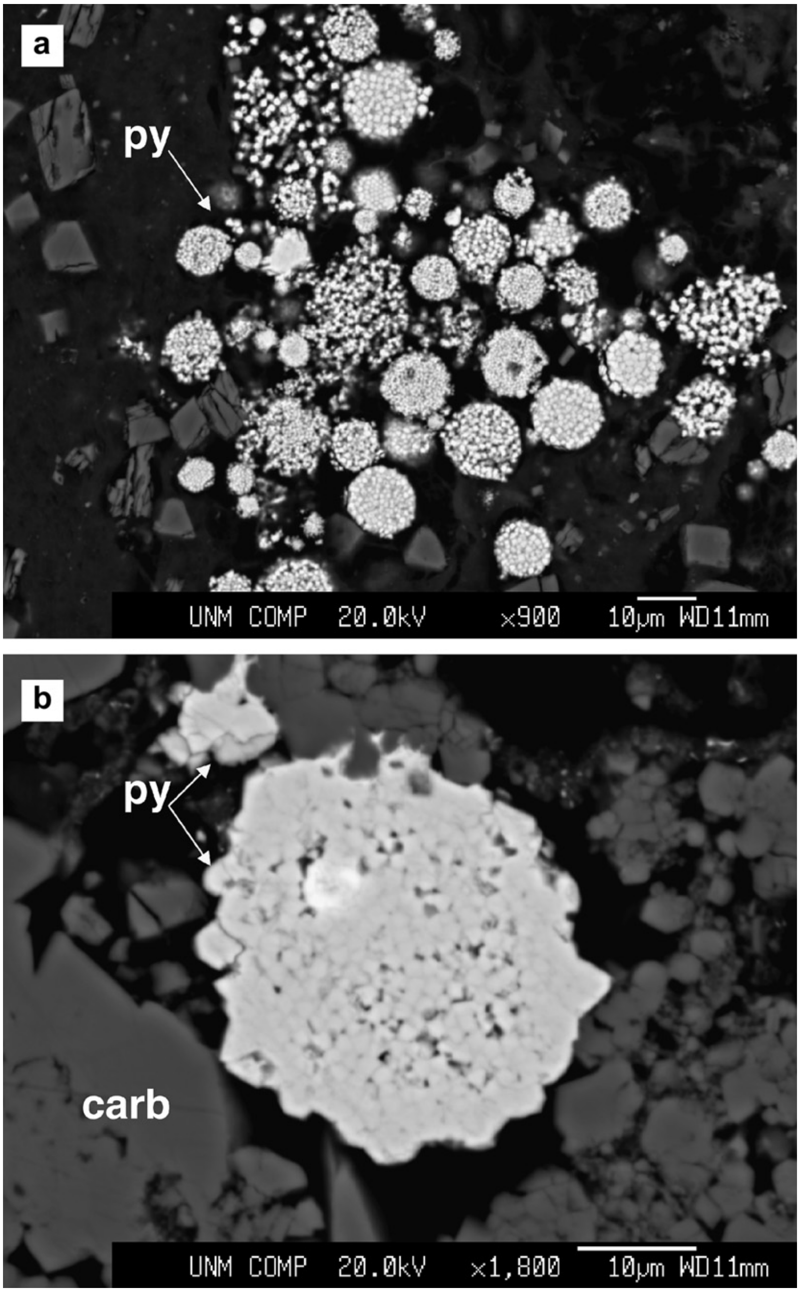

Fig. 3. Backscattered images of framboidal pyrite (py) in carbonate matrix (carb) from sample 20-143 (Arcadia Formation). Note: scale bar in lower right is 10 μm.

significant linear correlation for As in the Tampa Member sediments existed with S ($R^2 = 0.61$) (Fig. 9, Appendix 1).

The bulk As concentrations in sediments from the Nocatee Member of the Arcadia Formation ranged from 0.5 to as high as 69.0 mg/kg (Table 1). The mean value for 27 samples was 6.5 mg/kg ($\sigma = 13.1$ mg/kg). Approximately 88% of the samples contained less than 10 mg/kg As and roughly 22% less than 1 mg/kg. The sample 12-529 from the Nocatee Member was composed of greenish clay with a significant amount of pyrite (framboids) and represented the highest As concentration (69.0 mg/kg) of all Hawthorn Group samples. A high degree

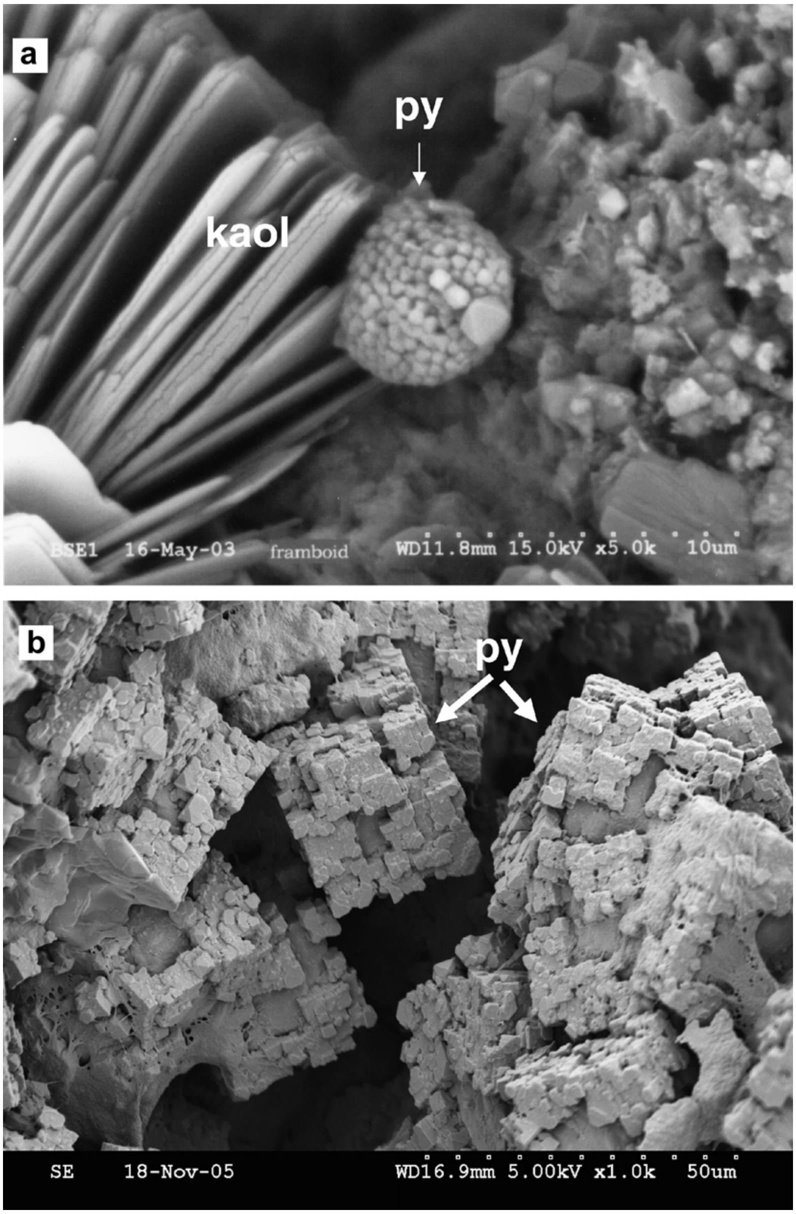

Fig. 4. Scanning electron micrographs of pyrite: (a) Framboidal pyrite (py) and kaolinite (kaol) in sample 22-170 from the Tampa Member (As concentration of the bulk sample is 14.0 mg/kg); note: scale bar in lower right is 10 μm. (b) Cubic pyrite (py) in sample 12-125(2) from the Peace River Formation (As concentration of the bulk sample is 26.7 mg/kg); note: scale bar in lower right is 50 μm.

of linear correlation for the Nocatee Member sediments existed for Fe with S ($R^2 = 0.85$), and Fe with Al ($R^2 = 0.81$) (Appendix 1).

3.2.2. Peace River Formation

The total As concentrations in samples from the Peace River Formation ranged from 0.4 to 40.8 mg/kg (Table 1). Mean value for 54 samples was 8.8 mg/kg ($\sigma = 8.6$ mg/kg). Approximately 70% of the samples had As concentrations less than 10 mg/kg and about 7% less than 1 mg/kg (Appendix 2). Samples consisting mostly of pure carbonates or sandstone with no visible trace minerals had low concentrations of As. Generally, high As concentrations occurred with pyrite, clay, HFO, and francolite.

The strongest linear correlation for the Peace Formation sediments existed between Fe and S

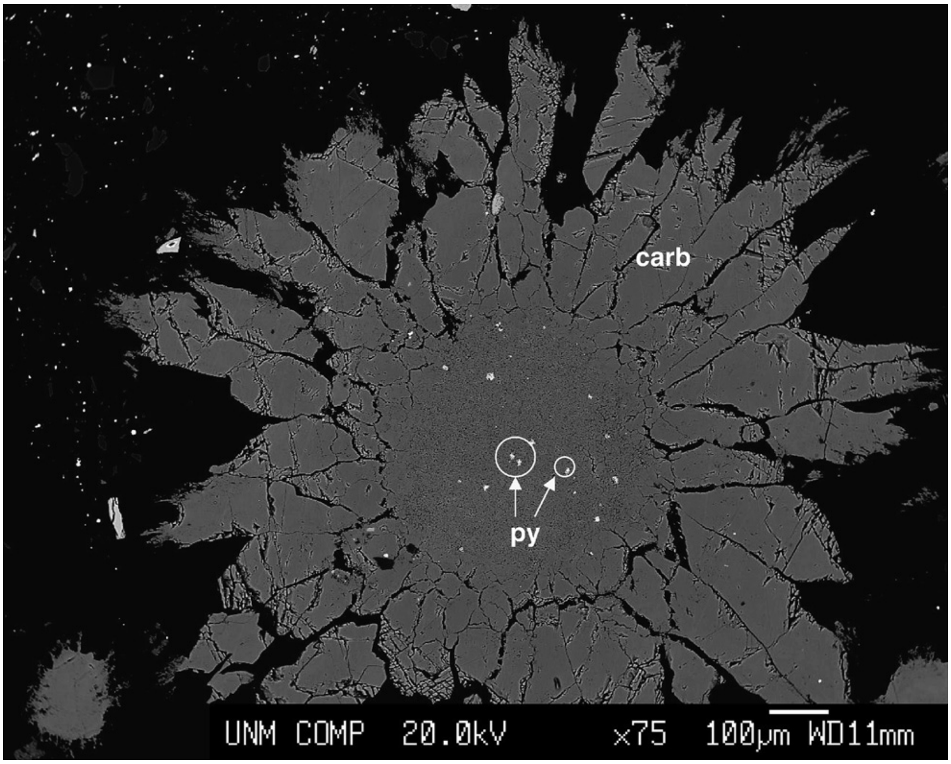

Fig. 5. Backscattered image of pyrite (py) (in circles) in calcite (carb) matrix in sample 12-48 (Peace River Formation) taken with the EMPA using a JEOL 8200.

Table 1
Maximum, minimum, mean and standard deviation of As concentrations in mg/kg for the Hawthorn Group and its Formations/Members

	Maximum	Minimum	Mean	Standard deviation	(*n*)
Hawthorn Group (all samples)	69.0	0.1	5.6	7.1	362
Hawthorn Group (interval samples)	40.8	0.1	5.0	5.8	285
Hawthorn Group ("special interest" samples)	69.0	0.4	8.3	10.5	77
Undifferentiated Arcadia Formation	36.0	0.1	5.7	6.2	205
Tampa Member	15.2	1.2	3.0	3.7	75
Nocatee Member	69.0	0.5	6.5	13.1	27
Peace River Formation	40.8	0.4	8.8	8.6	55

($R^2 = 0.94$) (Appendix 1), which could be due to the outlier effect caused by sample 12-125(2). Removing the outlier from the plot resulted in a significantly lower degree of linear correlation ($R^2 = 0.59$). This is because analyzed samples contained not only pyrite, but also contained HFO and gypsum, sources of Fe and S.

3.3. Occurrence of arsenic in matrix and individual minerals

After determination of bulk As concentrations samples with high As were selected for a more detailed geochemical and mineralogical investigation. The electron-probe (EMPA) analysis of 16 thin sections with variations in lithologic compositions revealed that substantial As concentrations were present only in pyrite. About 126 pyrite framboids were analyzed for As and concentrations ranged from <1 to 8260 mg/kg with a mean of 1272 mg/kg ($\sigma = 1379$ mg/kg) (Table 2). Prior studies of framboidal pyrite in the Suwannee Limestone, which underlies the Hawthorn Group, demonstrated a similar As enrichment in pyrite, ranging from 100 to 11 200 mg/kg (Price and Pichler, 2006).

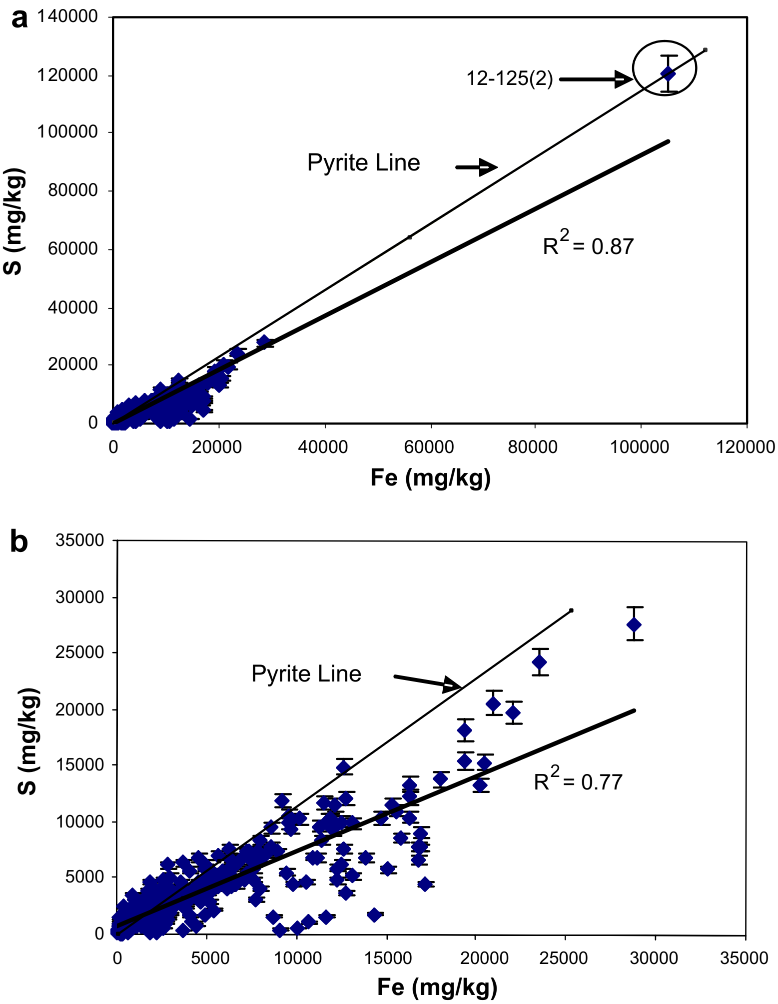

Fig. 6. (a) Correlation between Fe and S (in bold) for the Hawthorn Group all data ($n = 362$) analyzed by ICP-OES; (b) Correlation between Fe and S (in bold) after the outlier (12-125(2)) was removed. The "Pyrite line" represents pyrite dissolution as a source of Fe and S (Fe = 2S).

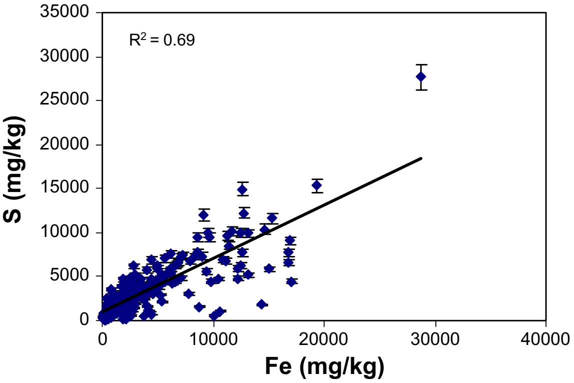

Fig. 7. Correlation between Fe and S (in bold) for the Hawthorn Group interval samples ($n = 285$).

The elemental maps of clays, pyrite, dolomite, quartz and francolite demonstrated that high concentrations of As were generally associated with pyrite and sometimes with HFO. The elemental map of a francolite nodule (sample 5-1-235, undifferentiated Arcadia Formation) revealed the presence of very small pyrite crystals (<5 μm) inside the nodule (Fig. 10). Arsenic values in these pyrites were up to 3700 mg/kg while As values in the phosphate matrix were <1 mg/kg. The elemental mapping of sample 4-1-501 from the undifferentiated Arcadia Formation demonstrated As enrichment in both pyrites and HFO, and showed a heterogeneous distribution of As.

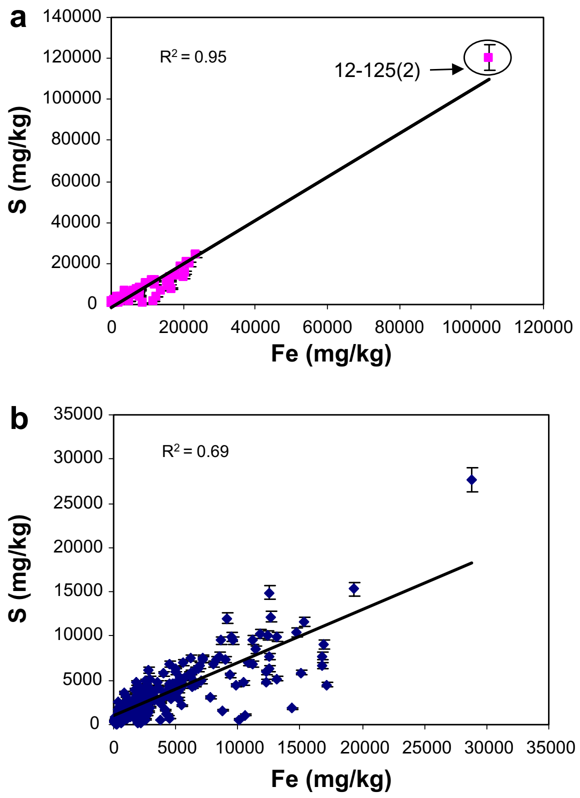

Fig. 8. (a) Correlation between Fe and S (in bold) for the Hawthorn Group "special interest" samples (samples likely to have high As concentrations; $n = 77$); (b) Correlation between Fe and S after the outlier (12-125(2)) was removed.

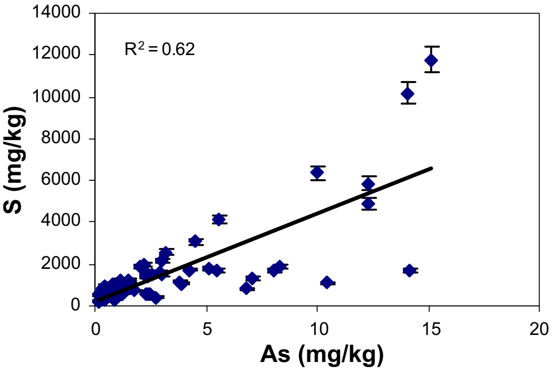

Fig. 9. Correlation between As and S for the Tampa Member of the Arcadia Formation.

The EMPA mapping of sample 12-125 from the Peace River Formation clearly showed the concentration of As in pyrite, compared to clay and phosphate materials (Figs. 11 and 12). For the bulk-rock analysis, sample 12-125 was divided into two parts due to its heterogeneity. Total As for sample 12-125(1) was 8.1 mg/kg and 26.7 mg/kg for 12-125(2) (Appendix 2). Sample 12-125(2) possibly represented a burrow fill with a significant amount of pyrite in the phosphate matrix.

The electron microprobe analysis of 31 pyrites in sample 22-170 (Tampa Member of the Arcadia Formation) clearly illustrated the large range of As concentrations over a small area. Values ranged from 10 to 2180 mg/kg. These results confirmed the extremely heterogeneous distribution of As not only between pyrite and other Hawthorn Group minerals, but also within pyrites themselves.

4. Discussion

The objectives of this study were to examine: (1) mineralogical association, (2) concentration, and (3) distribution of As in the Miocene Hawthorn Group in southwestern Florida. This research is essential for the planning of phosphate mining operations and forecasting As behavior in the subsurface during anthropogenic induced physico-chemical changes in the aquifer.

Arsenic occurred throughout the entire Hawthorn Group and concentrations varied drastically from formation to formation (Table 1). The distribution of As mean values for the each formation and member of the Hawthorn Group showed a decrease of As concentration with depth (Fig. 13). The same distribution patterns occurred for Fe, S, Al, and P (Fig. 14). According to Scott (1988), the siliciclastic components, such as clay, francolite, and quartz sand are dominant in the Peace River Formation and their role in the Hawthorn Group decreases with depth. Therefore, the overall decrease of As concentrations with depth correlated to the siliciclastic content. Only the Nocatee Member of the Arcadia Formation revealed a higher mean As concentration, which could be due to the outlier effect (Swan and Sandilands, 1995) caused by sample 12-529, which had the highest As concentration of all Hawthorn Group samples (69 mg/kg) (Fig. 13a). Elimination of the outlier resulted in a lower As mean value (4.1 mg/kg) for the Nocatee Member (Fig. 13b). The higher contribution of siliciclastic material in the Nocatee Member (Scott, 1988) demonstrated the elevated values of Fe, S, Al and P compared to those in the Tampa Member (Fig. 14).

4.1. *Potential sources of arsenic in the Hawthorn Group*

There are four major potential sources of As in the Hawthorn Group sediments:

Table 2
Electron microprobe results for As concentration in pyrites for the Formation/Member of the Hawthorn Group (in mg/kg)

	Maximum	Minimum	Mean	Standard deviation	(*n*)
Hawthorn Group (all analyzed pyrites)	8260	<1	1272	379	126
Undifferentiated Arcadia Formation	8260	< 1	1437	1569	48
Tampa Member	3220	<1	1004	770	39
Nocatee Member	5710	560	2884	1896	9
Peace River Formation	4160	<1	772	1082	30

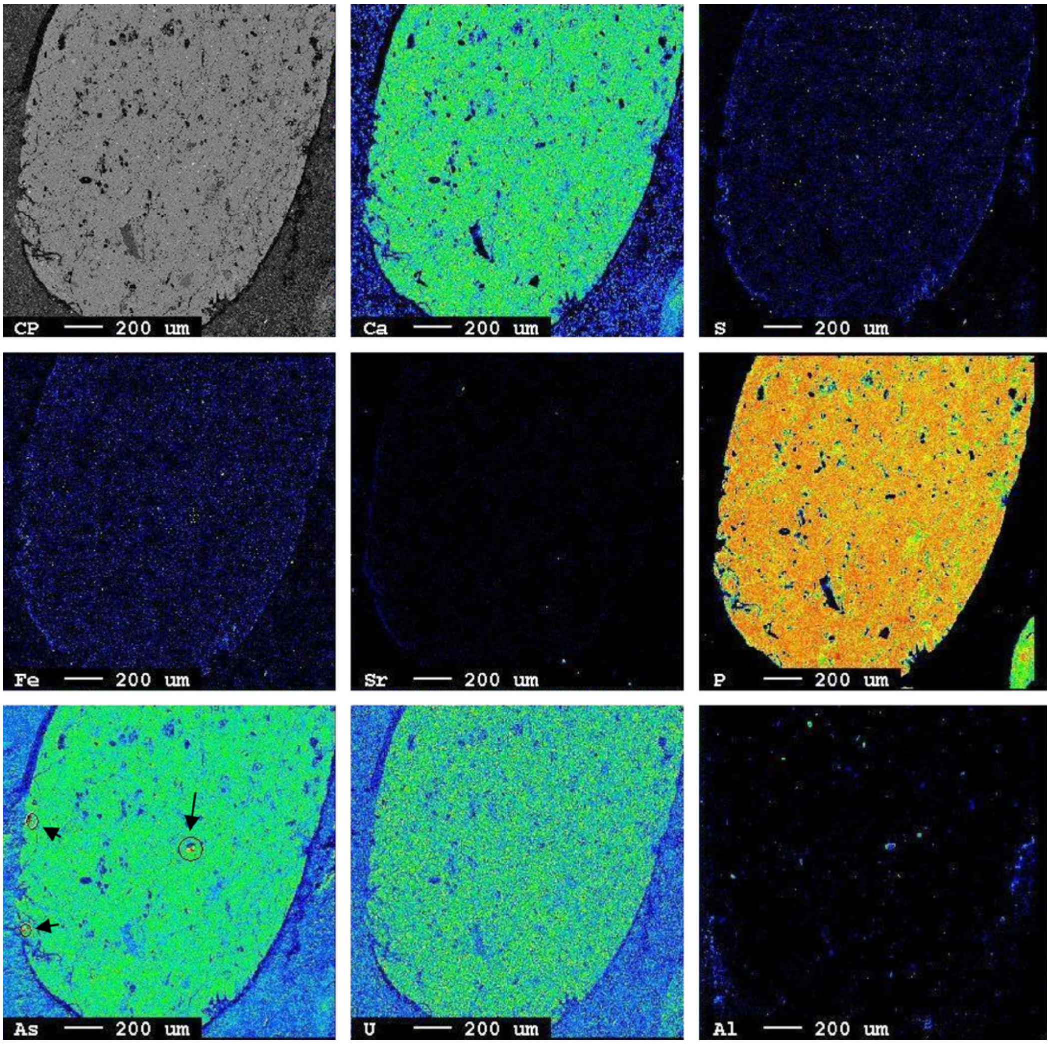

Fig. 10. Elemental mapping of francolite grain in sample 5-1-235 (undifferentiated Arcadia Formation). Note black circles on As map represent the enrichment of As concentration in pyrites. Background was not subtracted; relative concentrations increase with a change in color from blue to yellow to red.

(1) Substitution at any of the fluorapatite sites in francolite;
(2) Substitution in the crystal structure of sulfide minerals, such as pyrite and arsenopyrite;
(3) Adsorption or ion exchange onto clay and organic matter;
(4) Adsorption or coprecipitation with HFO.

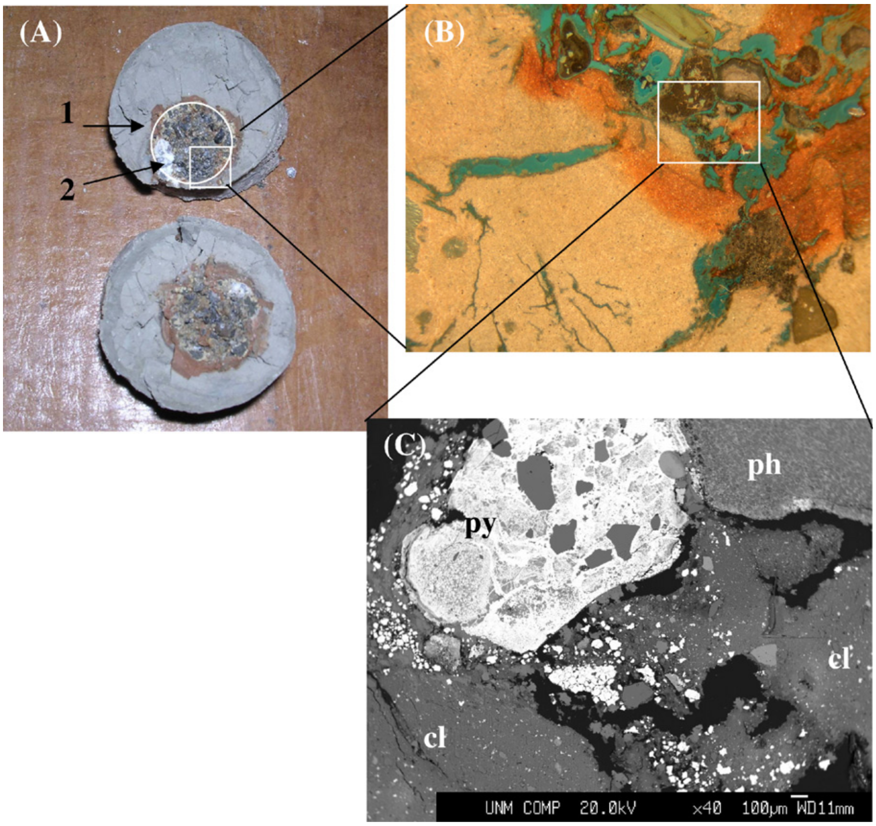

Fig. 11. (A) Photograph of sample 12-125 (Peace River Formation) composed of clays (1 = 12-125(1)) and pyrite – phosphate matrix (2 = 12-125(2)); (B) Photomicrograph of contact between sample (1) and (2); (C) Backscattered image of pyrite (py), clay (cl) and phosphate (ph).

4.1.1. *Francolite (carbonate fluorapatite)*

The highly open crystal structure of francolite permits substitution at any of the fluorapatite sites, e.g. Na^+, Mg^{2+}, Sr^{2+} for Ca^{2+}; OH^-, AsO^{3-}, CrO^{2-}, VO^{3-} for PO_4^{3-}; and Cl^-, Br^- for F^- (Shields, 2002). According to Smedley and Kinniburgh (2002), Ca phosphate or apatite can contain up to 1000 mg/kg As. On the other hand, Stow (1969) did not report any correlation between As and P in the Bone Valley Member of the Hawthorn Group. The combination of the ICP-OES and HG-AFS showed no correlation between As and P. However, the EMPA elemental mapping of the internal chemical composition of the francolite nodule from the undifferentiated Arcadia Formation revealed the occurrence of pyrite inclusions with As enrichment as high as 3700 mg/kg compared to phosphate matrix with As of <1 m/kg (Fig. 10).

4.1.2. *Pyrite*

Detailed lithologic examinations of the Hawthorn Group sediments with a stereo and scanning electron microscope revealed the existence of unevenly distributed pyrite occurring mostly with greenish clays, francolite and organic material. The majority of pyrite in the Hawthorn Group samples was present in the form of framboids, cubic pyrite only occurred in one sample (Fig. 4b). According to Ohfuji and Rickard (2005) framboidal pyrite is a microscopic spheroidal to sub-spheroidal aggregate with an internal microcrystalline structure and a distinctive raspberry-like shape. Price and Pichler (2006) reported that pyrite in the Suwannee Limestone, which directly underlies the Hawthorn Group sediments, was mostly present as pseudo-framboids, or framboid-shaped pyrite aggregates. Massive internal structure of pseudo-framboidal pyrite is composed of interlocking granular or acicular pyrite microcrystals (Ohfuji and Rickard, 2005; Wang and Morse, 1996).

Examination of thin sections with the polarizing microscope demonstrated that framboidal pyrites occurred in about 90% of all samples as a trace mineral in the sediment matrix and as inclusions in

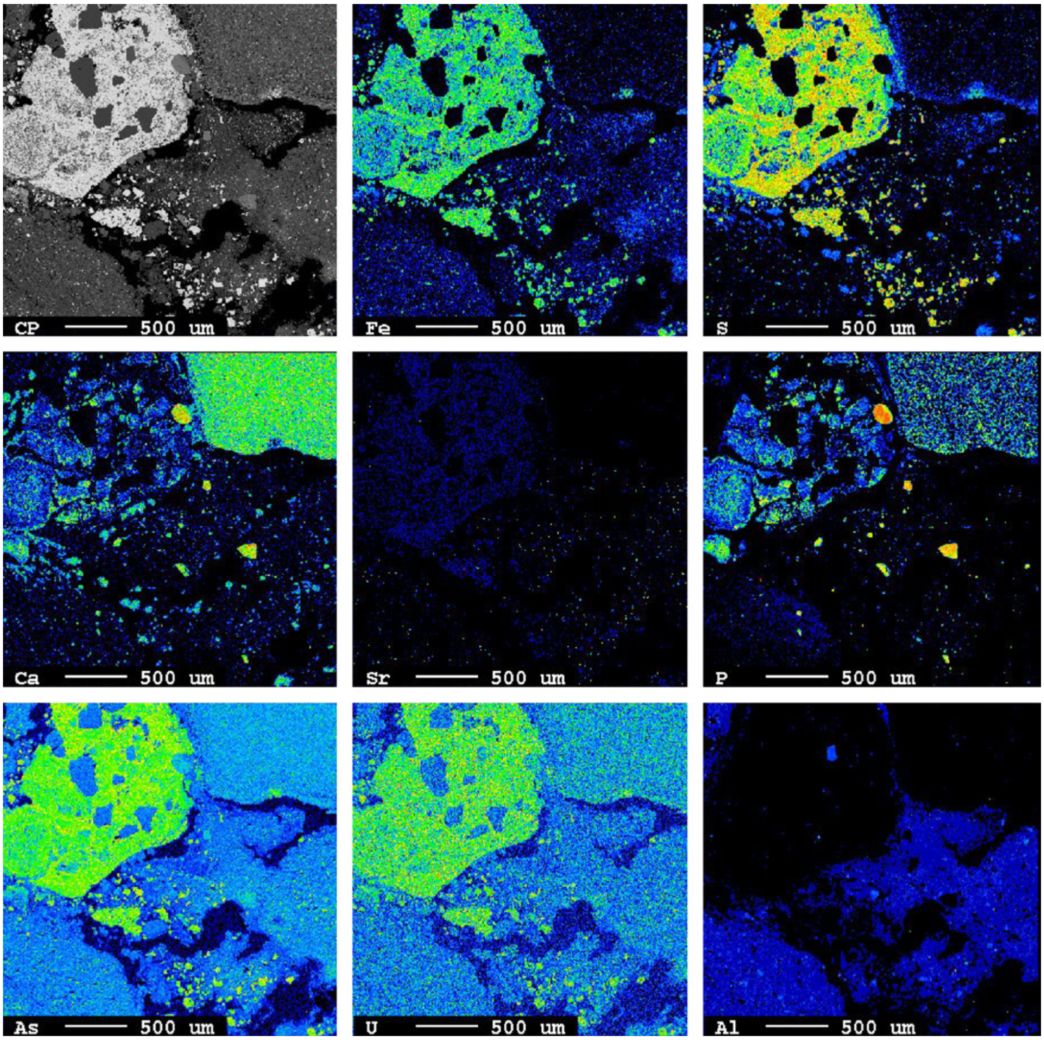

Fig. 12. Elemental mapping of pyrite in sample 12-125 (Peace River Formation). Note increase of As concentration in pyrite compare to matrix. Background was subtracted; relative concentrations increase with a change in color from blue to yellow to red.

francolite grains and calcite crystals. Prior studies of sulfide minerals such as the abundance and occurrence of pyrite in the Suwannee Limestone (Price and Pichler, 2006) revealed significant enrichment of As in pyrite with concentrations as high as 11 200 mg/kg. Thomas and Saunders (1998) reported As concentrations in pyrite framboids of up to 1000 mg/kg as a substitute element for S in the FeS_2 structure. Huerta-Diaz and Morse (1990, 1992) found As concentrations in marine sedimentary pyrites of up to 9300 mg/kg. Therefore, sedimentary pyrite can be a significant sink and potential source of As.

The ICP-OES results revealed a strong linear correlation between S and Fe ($R^2 = 0.87$) confirming the presence of pyrite (Fig. 6). Lack of a significant correlation between As and S or Fe was probably due to the contribution of As from other sources, such as clays, HFO, francolite, or organic matter. The electron microprobe analyses of 16 thin sections with variations in lithologic composition revealed that substantial As concentrations were present in pyrite. Arsenic concentrations in 126 analyzed pyrites ranged from <1 to as high as 8260 mg/kg showing the heterogeneous distribution of As (Table 2).

4.1.3. *Clay and organic matter*

Clay minerals readily adsorb As because of the oxide-like character of the edges of their crystals (Goldberg, 2002). The lithologic examination of

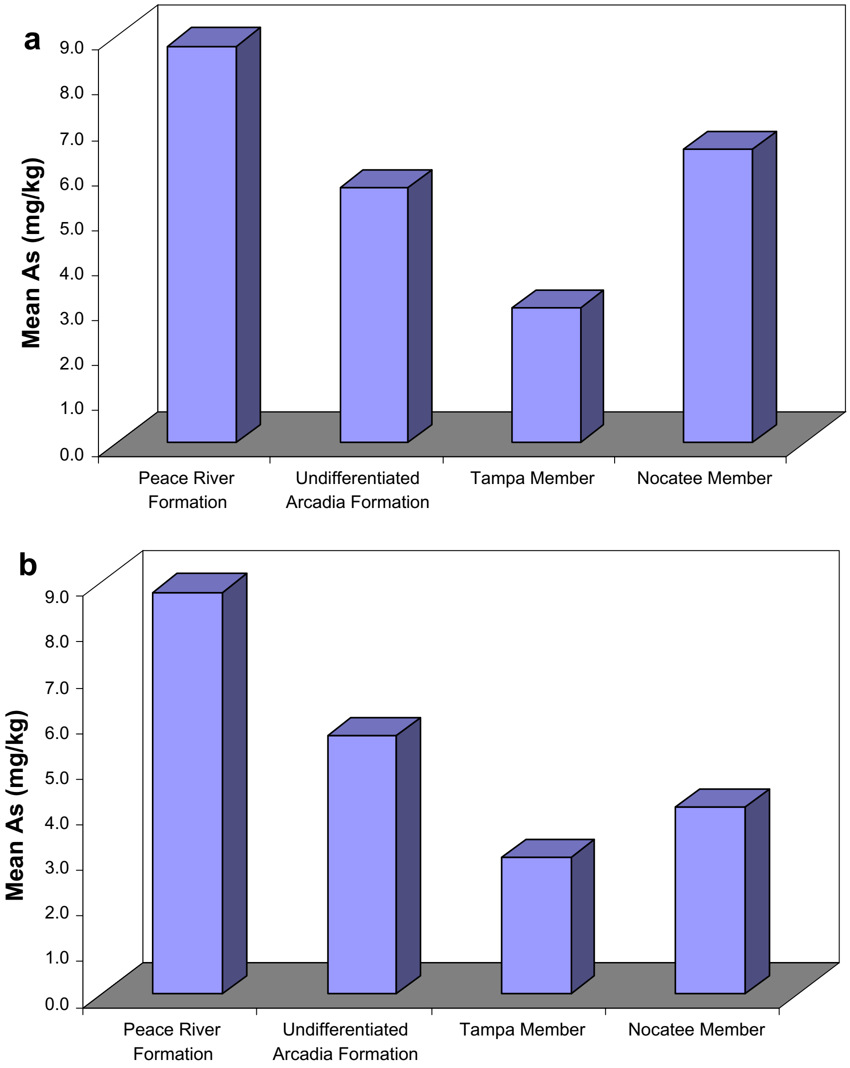

Fig. 13. (a) Distribution of the mean As concentrations throughout the Hawthorn Group all data ($n = 362$); (b) Distribution of the mean As concentrations without the outlier.

the Hawthorn Group sediments revealed the abundance of green or brownish green clays mostly in the Peace River Formation. Generally, green clays contained unevenly distributed pyrite and francolite. The HG-AFS analyses of clays generally showed high As concentrations. Organic matter has a very small particle size, which, therefore, results in a large surface area per unit volume and ability to adsorb As. Moreover the potential of organic material to generate complexes with heavy metals is due to the existence of O-containing functional groups such as carboxyl (COOH), hydroxyl (OH), and carbonyl (C=O) (Evangelou, 1995). The study of Compton et al. (2002) demonstrated that phosphorite grains can contain inclusions of organic matter, clay minerals, pyrite, quartz and biogenic calcite. Detailed lithologic examinations of the Hawthorn Group samples revealed the abundance of organic matter mostly in the Arcadia Formation. The HG-AFS analysis of samples with organic matter revealed As concentration of about 5 mg/kg. At the same time, concentrations of As in samples containing green clays with pyrite was as high as 69 mg/kg.

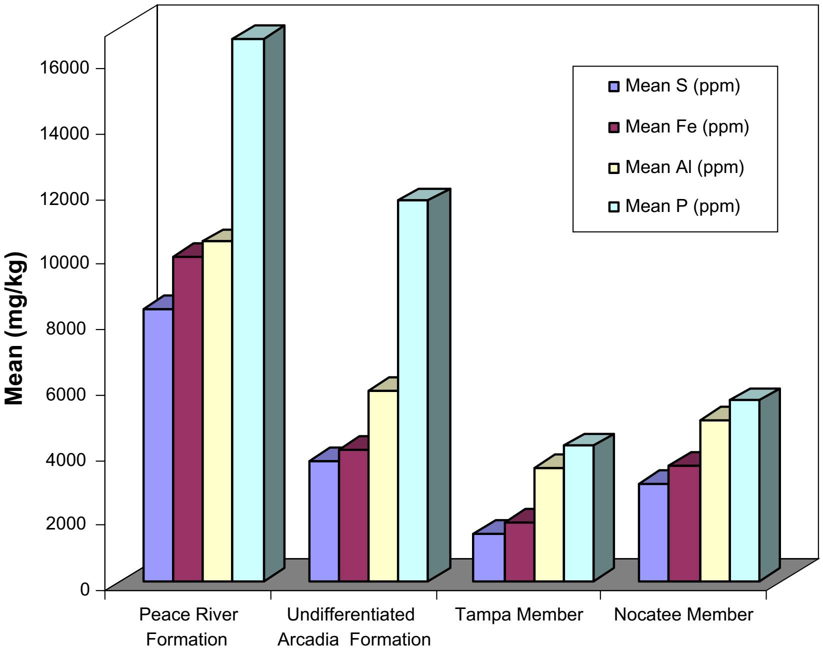

Fig. 14. Distribution of the mean S, Fe, Al and P concentrations throughout the Hawthorn Group all data ($n = 362$).

4.1.4. Hydrous ferric oxides (HFO)

It has been shown that As incorporates into sediments by co-precipitation with HFO, or is adsorbed onto the extremely high surface area of precipitated HFO (Hongshao and Stanforth, 2001; Evangelou, 1995; Pichler et al., 1999). The close connection between HFO and As is well documented (e.g., Pichler et al., 2001; Pichler and Veizer, 1999). Stow (1969) reported that most of the As in the Bone Valley Member of the Hawthorn Group was adsorbed onto HFO. Detailed lithologic examinations revealed the occurrence of HFO throughout the Hawthorn Group as stains or rings around pyrites. According to Compton et al. (1993) reworking of the Hawthorn Group sediment during periods of marine regressions caused oxidation of some pyrite and formation of HFO. The electron microprobe analysis showed that HFO from the undifferentiated Arcadia Formation contained up to 540 mg/kg As.

4.2. Quantified role of pyrite

It appears that framboidal pyrite contained the majority of As in the Hawthorn Group. This can be verified by a simple mass balance approach using the bulk concentrations of Fe, S and As combined with As concentrations in individual pyrites. Due to the strong linear correlation between S and Fe ($R^2 = 0.87$), it is conceivable that Fe and S in Hawthorn Group samples are controlled largely by the presence of pyrite. The pyrite line (Fe = 2S) represents Fe/S ratios that are exclusively controlled by pyrite (Fig. 6). Thus, using the values of S and Fe, the abundance of pyrite in each sample was calculated. Then, the calculated amount of pyrite was multiplied by the mean As concentration in pyrite of each analyzed thin section and compared to the actual analyzed bulk As concentrations (Table 3). Calculated and measured As were compared in Fig. 15. For those samples that lie significantly above the equal concentration line, calculated As concentrations were lower than those measured in the bulk sample (Fig. 15). These results can be explained by existence of other sources of As (clays, francolite, organic material, HFO) or underestimation of the possible amount of pyrite, or an insufficient number of analyzed pyrite crystals. Sample 49-154.5 showed much higher calculated As concentration compared to a measured result probably due to overestimation of pyrite constituent or an insufficient number of analyzed pyrites.

4.3. Mobilization of arsenic during phosphate mining

Apatite group minerals are stable under a broad range of geologic conditions for millions of years (Wright, 1990; Nriagu, 1974). The trace elemental composition of the apatite fossil teeth and bones, and analyses of the sedimentary phosphorite deposits by Wright (1990) and others (Keto and Jacobsen, 1987; Shaw and Wasserburg, 1985) has revealed that biogenic and sedimentary apatite incorporates considerable amounts of radionuclides and metals from seawater. Different elements substitute for Ca, PO_4 and OH in the apatite crystal structure (Skinner and Catherine, 2002). Apatite locks these metals and radionuclides in a crystal structure for up to a billion years with no consequent leaching, exchange or desorption, even due to diagenetic changes in water chemistry, pH and temperatures. This is because the apatite mineral structure is very stable in a broad range of environmental conditions, such as pH 2 to 12, temperature as high as 1000 °C, and the presence of aqueous and non-aqueous solutions (Shields, 2002). Studies of the carbonate fluorapatite, francolite by McConnell (1973), Jahnke (1984) and Regnier et al. (1994) however suggest that the substitution of CO_3^{2-} in carbonate fluorapatite leads to the destabilization of its crystal structure and, therefore, increase in solubility.

The Peace River Formation of the Hawthorn Group contains substantial amounts of francolite and is currently being exploited for phosphate ore. According to the present study, the Peace River Formation contained the highest concentration of As ($\mu = 8.8$ mg/kg) in the Hawthorn Group (Table 1). Detailed mineralogical analyses have confirmed the presence of ubiquitous framboidal pyrites harboring considerable amounts of As. In addition, EMPA elemental mapping has revealed that pyrite crystals were located both inside the francolite matrix with As as high as 3730 mg/kg (Fig. 10) and as a trace mineral in the sediment matrix with varying concentrations.

Because of the complicated distribution of pyrite in the Hawthorn Group, there are several potential scenarios that could lead to the mobilization of As during phosphate mining: (1) Oxidation of pyrite under aerobic conditions that could cause the release of substantial amounts of SO_4,

Table 3
Calculated As concentrations in pyrite compared to measured bulk As concentrations

Sample	Hawthorn Fm/Mm[a]	S (mg/kg)	Fe (mg/kg)	FeS_2 (mg/kg)	FeS_2 (%)	Mean As measured in pyrite (mg/kg)	(*n*)	As calculated in pyrite (mg/kg)	As measured in bulk (mg/kg)
9-30	PR	4479	3905	8384	1	1337	15	11	41
13-195	PR	7545	6579	14124	1	688	4	10	18
12-48	PR	5833	5086	10919	1	15	4	0	3
20-215	AF	7293	6358	13651	1	1096	10	15	36
20-143	AF	7429	6477	13906	1	2570	11	36	32
49-154.5	AF	10569	9210	19773	2	2620	3	52	28
5-1-235	AF	7350	6408	13758	1	1468	8	20	17
25-299	AF	9356	8158	17514	2	1734	5	30	28
4-1-501	AF	2839	2475	5314	1	186	5	1	1
5-320	AF	9595	8365	17960	2	34	5	1	24
22-170	AF	10190	8883	19073	2	929	31	18	14
3-3-275	AF	4892	4265	9157	1	2036	5	19	12
12-529	NM	13805	12036	25841	3	2884	9	75	69

[a] Hawthorn Group Formation/Member: PR – Peace River Formation, AF – Arcadia Formation, NM – Nocatee Member, (*n*) – number of pyrites in each thin section.

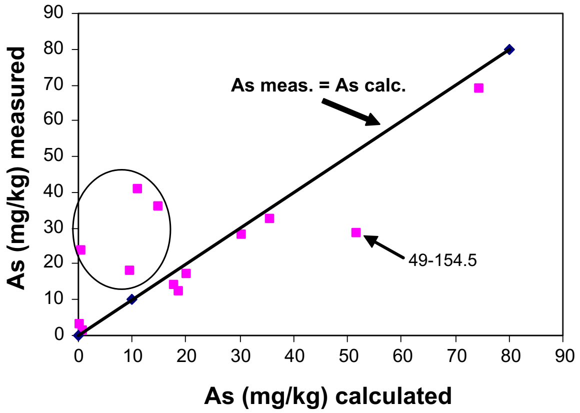

Fig. 15. Arsenic calculated vs. As measured from the Hawthorn Group. For samples in circle that lie significantly above the equal concentration line, calculated As concentrations were lower than those measured in the bulk. Sample 49-154.5 showed much higher calculated As concentration compared to a measured result probably due to overestimation of pyrite constituent or an insufficient number of analyzed pyrites.

acids and As (Smedley and Kinniburgh, 2002). Furthermore, these releases could lead to contamination of water supplies, pollution of rivers and bays in Florida, affecting aquatic life; and (2) breakdown of francolite nodules that contain As-enriched pyrite during phosphate ore processing.

Arsenic enrichment can cause several latent problems for the phosphate industry. First of all, As can be a significant toxin to livestock. There have been several incidences of swine fatalities due to As poisoning as a result of phosphate feed additives (El Bahri and Romdane, 1991). Additionally, the use of phosphates as fertilizers influences the release of As and enhances its mobility (Peryea, 1991). Arsenate and phosphate behave chemically similar and therefore, compete for binding sites in the soil. Phosphate addition to soils, for example, can enhance As release from specific sorption sites in soil through competitive anion exchange (Peryea and Kammereck, 1997).

5. Conclusions

(1) arsenic content of the Hawthorn Group varied from formation to formation and was mostly concentrated in pyrite;
(2) average As concentrations significantly changed from 8.8 mg/kg in the Peace River Formation to 3.0 mg/kg in the Tampa Member of the Arcadia Formation. Arsenic concentrations for all Hawthorn samples varied from 0.1 to 69.0 mg/kg;
(3) pyrite, with the exception of one out of 362 samples, occurred as framboids and was unevenly distributed throughout the Hawthorn Group;
(4) pyrite framboids were located inside the francolite matrix with As as high as 3730 mg/kg and as a trace mineral in the sediment with concentrations varying from <1 mg/kg to 8260 mg/kg;
(5) hydrous ferric oxides contained As as high as 540 mg/kg;
(6) francolite, organic material, and clays contained low As concentrations compared to pyrite;
(7) arsenic enrichment in phosphate nodules contained in the Peace River Formation could pose a potential problem for the phosphate industry, because high As values in the phosphate-bearing rock can have a negative effect on ore processing and the quality of the final product;
(8) mining induced release of As from the Peace River Formation is an environmental concern that warrants additional studies.

Acknowledgements

The project was funded through a grant to TP from the Southwest Florida Water Management District. We would like to thank Drs. Jonathan Arthur, Peter Harries, Gregg Jones and Thomas Scott for reviewing the manuscript and providing valuable suggestions. Mike Spilde is thanked for his help with the EMPA analysis at the University of New Mexico. The core material for this project was provided by the Florida Geological Survey in Tallahassee, Fl.

Appendix 1

Correlation matrices for (A) the Hawthorn Group all data (362 samples); (B) 285 interval samples; (C) 77 “special interest” samples; (D) 205 samples from the undifferentiated Arcadia Formation; (E) 75 samples from the Tampa Member, and (F) 27 samples from the Nocatee Member. Significant correlations are in bold.

	Ca	Fe	Mg	Mn	Si	S	P	Al	As
(*A*)									
Ca	1	−0.43	−0.13	−0.24	−0.29	−0.27	−0.12	−0.64	−0.29
Fe		1	−0.03	0.38	0.25	**0.87**	0.27	0.57	0.35
Mg			1	0.23	0.09	−0.01	<0.01	0.04	0.04
Mn				1	0.11	0.30	0.36	0.41	0.27
Si					1	0.22	0.28	0.24	0.28
S						1	0.29	0.35	0.40
P							1	0.28	0.14
Al								1	0.25
As									1
(*B*)									
Ca	1	−0.55	−0.17	−0.24	−0.25	−0.4	−0.16	−0.59	−0.09
Fe		1	0.04	0.47	0.31	**0.69**	0.30	0.63	0.32
Mg			1	0.27	0.09	0.09	−0.02	0.07	0.01
Mn				1	0.15	0.42	0.38	0.42	0.07
Si					1	0.37	0.32	0.26	0.06
S						1	0.37	0.35	0.26
P							1	0.33	0.19
Al								1	0.25
As									1
(*C*)									
Ca	1	−0.11	<0.01	−0.07	−0.12	−0.05	<0.01	−0.48	−0.05
Fe		1	0.03	0.2	0.04	**0.95**	0.08	0.15	0.17
Mg			1	0.03	<0.01	0.003	<0.01	<0.01	<0.01
Mn				1	<0.01	0.16	0.07	0.20	0.11
Si					1	0.03	0.06	0.02	0.10
S						1	0.11	0.06	0.13
P							1	0.02	0.10
Al								1	0.15
As									1
(*D*)									
Ca	1	−0.46	−0.17	−0.19	−0.28	−0.32	−0.06	−0.51	−0.14
Fe		1	−0.06	0.38	0.18	**0.81**	0.14	**0.74**	0.30
Mg			1	0.19	−0.01	−0.08	−0.11	−0.03	<0.01
Mn				1	0.03	0.37	0.33	0.35	0.12
Si					1	0.18	0.23	0.23	0.02
S						1	0.27	0.51	0.28
P							1	0.21	0.10
Al								1	0.35
As									1
(*E*)									
Ca	1	−0.52	−0.27	−0.18	−0.28	−0.34	−0.29	−0.58	−0.17
Fe		1	0.24	0.44	0.19	**0.63**	0.51	**0.76**	0.53
Mg			1	0.54	0.23	0.24	0.03	0.22	0.11
Mn				1	0.25	0.30	0.05	0.29	0.23
Si					1	0.16	0.08	0.16	0.23

Appendix 1 (*continued*)

	Ca	Fe	Mg	Mn	Si	S	P	Al	As
S						1	0.58	0.78	0.61
P							1	0.48	0.16
Al								1	0.55
As									1
(*F*)									
Ca	1	−0.44	−0.12	−0.39	−0.28	−0.38	−0.01	−0.36	−0.08
Fe		1	0.25	**0.77**	0.50	**0.85**	0.03	**0.81**	0.49
Mg			1	0.31	−0.05	0.13	0.29	0.42	<0.01
Mn				1	0.58	0.61	0.10	0.45	0.11
Si					1	**0.74**	0.16	0.44	0.61
S						1	0.12	0.51	0.51
P							1	0.05	<0.01
Al								1	0.28
As									1

Appendix 2

Inductively coupled plasma – optical emission spectrometry (ICP-OES) and hydride generation-atomic fluorescence spectrometry (HG-AFS) results for the Peace River Formation samples sorted by well (concentrations in mg/kg)

Sample	Ca	Fe	Mg	Mn	Si	S	P	Al	As
39-47.5-52.5	<0.01	264	<0.01	2.5	133	55	326	761	0.4
39-72.5-77.5	42920	2284	<0.01	44.8	851	1713	17667	2019	8.1
39-100	28872	12223	20962	84.6	347	4814	8117	19635	6.1
39-125	116704	4712	61947	148.8	308	3800	9277	8131	4.3
39-130	52157	15487	16759	99.6	383	11014	6760	19303	6.5
39-150	82302	14666	56559	259.9	652	10390	7504	21844	6.1
39-155	80199	8075	22954	140.5	347	6876	15143	14436	5.3
39-173-178	58628	3258	1892	55.9	623	3065	20941	3512	5.9
22-20	168057	14362	2187	85.2	2376	1825	55029	12217	11.2
22-29	22989	9004	5216	28.2	449	487	8036	11465	5.3
22-45	155462	11164	90636	184.9	416	6815	8929	14106	9.3
30-Sep	45277	17101	10695	30.4	242	4479	12602	23236	40.8
25-45-47	59901	1520	<0.01	14.9	1347	1292	22199	4550	4.5
25-65-70	220330	15330	48352	97.3	1645	11597	48881	13462	37.2
25-90	268317	7178	97030	106.4	1503	7327	41624	9307	13.1
TR-9-2-40	39167	12500	44510	98.5	2892	6275	7404	18873	4.0
20-38.5	206198	5822	15018	47.1	3583	5632	60253	3033	12.2
20-48.5	16834	16283	13377	37.6	894	13379	4801	12826	9.8
20-65	250873	2509	140861	50.6	666	2466	1842	1857	1.9
17-50-56	353922	6176	27941	209.8	1407	4142	29614	4382	9.7
17-70	148529	13088	40882	455.4	859	9901	34632	13824	9.4
DV-1-6	<0.01	8	<0.01	<0.01	56	103	161	1414	1.3
DV-1-25-26	66162	1889	<0.01	27.3	954	200	50000	46212	1.1

(*continued on next page*)

Appendix 2 (*continued*)

Sample	Ca	Fe	Mg	Mn	Si	S	P	Al	As
DV-1-48.5-51	92929	10606	30455	127.3	1228	1080	22149	16061	3.0
DV-1-74.5-77	118182	8737	34899	123.7	898	1589	20778	14596	11.4
TR-3-3-56.5-61	121086	5376	13413	64.2	1986	5213	34453	2056	25.8
TR-3-3-81.5-86.5	187289	5304	61867	75.9	910	5059	23509	4235	13.9
49-77.3-82.3	85396	5365	8911	131.8	830	4292	25338	5662	14.9
13-19	12537	2605	<0.01	1.5	507	590	5561	10634	0.4
13-23	25248	11584	5644	18.8	2361	1629	8465	13366	0.4
13-45	180930	11395	23116	45.6	488	8465	4130	12093	8.2
13-69	180556	2778	101389	68.1	340	1421	852	4384	0.9
13-95	207407	2644	100926	19.9	1014	3556	755	1935	8.4
13-108	233659	883	118049	14.6	247	2127	737	756	3.2
13-120	171759	2898	81944	29.6	348	4106	2139	4120	3.3
13-134	25099	3040	7822	20.8	435	3327	3891	4272	1.1
13-145	167123	2904	49772	61.6	1187	5160	19909	3740	10.2
13-170	95434	9498	17991	125.6	498	9954	21781	16164	8.7
13-195	185455	6182	89545	78.2	1577	7545	12727	7636	17.7
4-1-50	46364	4441	<0.01	21.4	1405	4291	16318	4091	5.4
5-69-74	317561	9171	16976	25.9	2180	12000	52195	8585	20.0
9-85	76852	10185	10741	24.1	3204	10324	4347	11944	5.4
9-95	82938	12559	14313	28	3043	14929	5782	13223	3.8
5-110	69159	7944	6168	24.8	2047	8364	14019	9533	3.2
5-120	260550	8578	10550	24.3	1904	9495	33761	10000	25.1
12-41	36864	19364	16727	40.5	3355	15364	3323	15500	5.6
12-48	206019	7593	10000	38	3454	5833	1755	8565	2.9
12-64.5	377251	2564	5735	3.8	468	3370	383	133	2.1
9-90	208057	1640	106635	19.4	1858	1972	1019	1649	1.8
12-115	89450	7202	45000	65.1	2271	7431	2743	8486	3.9
12-125(1)	55721	23483	40149	167.7	557	24279	4836	20149	7.7
12-125(2)	161692	104975	9254	140.8	2209	120398	52736	5970	26.7
12-125(1)dup	56098	20976	43268	173.7	416	20585	4927	20585	8.1
12-140	106849	12694	47032	206.4	3169	12192	10091	14795	11.8
12-165	119444	7963	23611	263	1750	6806	27778	17639	6.2

References

Blakey, A.F., 1973. The Florida Phosphate Industry: A History of the Development and Use of a Vital Mineral. Harvard University Press, Cambridge.

Compton, J.S., Hodell, D.A., Garrido, J.R., Mallinson, D.J., 1993. Origin and age of phosphorite from the south-central Florida Platform: Relation of phosphogenesis to sea- level fluctuations and d13C excursions. Geochim. Cosmochim. Acta 57, 131–146.

Compton, J.S., Mulabisana, J., McMillan, I.K., 2002. Origin and age of phosphorite from the Last Glacial Maximum to Holocene transgressive succession off the Orange River. South Africa. Mar. Geol. 186, 243–261.

ElBahri, L., Romdane, S.B., 1991. Arsenic poisoning in livestock. Vet. Human Toxicol. 33, 259–264.

Evangelou, V.P., 1995. Pyrite Oxidation and Its Control. CRC Press, Boca Raton, Florida.

Goldberg, S., 2002. Competitive adsorption of arsenate and arsenite on oxides and clay minerals. Soil Sci. Soc. Am. J. 66, 413–421.

Green, R.C., Arthur, J.D., DeWitt, D., 1995. Lithostratigraphic and hydrostratigraphic cross sections through Pinellas and Hillsborough counties, Southwest Florida, Open File Report – Florida Geol. Surv. 61.

Hammett, Y.C., 2002, Coronet Working To Control Arsenic. Tampa Tribune, 30 December.

Hodges, A., Mulkey, D., Philippakos, E., 2001. Economic Impact of Florida's Agricultural Chemical and Mining Industries. Department of Food and Resource Economics, Institute of Food and Agricultural Sciences, University of Florida.

Hongshao, Z., Stanforth, R., 2001. Competitive adsorption of phosphate and arsenate on goethite. Environ. Sci. Technol. 35, 4753–4757.

Huerta-Diaz, M.A., Morse, J.W., 1990. Geochemistry of trace metals associated with sedimentary pyrite from anoxic marine sediments. Eos. Trans. Am. Geophys. Union 71 (2), 98.

Huerta-Diaz, M.A., Morse, J.W., 1992. Pyritization of trace metals in anoxic marine sediments. Geochim. Cosmochim. Acta 56, 2681–2702.

Jahnke, R.A., 1984. The synthesis and solubility of carbonate fluorapatite. Am. J. Sci. 284, 58–78.

Keto, L.S., Jacobsen, S.B., 1987. Nd and Sr isotopic variations of early Paleozoic oceans. Earth Planet. Sci. Lett. 84, 27–41.

McConnell, D., 1973. Apatite, Its Crystal Chemistry, Mineralogy, and Geologic and Biologic Occurrences. III. Springer-Verlag, Berlin.

Miller, J.A., 1986. Hydrogeologic framework of the Floridan aquifer system in Florida and in parts of Georgia, South Carolina, and Alabama. U.S. Geol. Surv. Prof. Pap. P 1403-B, B1-B91.

Nriagu, 1974. Lead orthophosphates, IV. Formation and stability in the environment. Geochim. Cosmochim. Acta 38, 887–898.

Ohfuji, H., Rickard, D., 2005. Experimental syntheses of framboids-a review. Earth Sci. Rev. 71, 147–170.

Peryea, F.J., 1991. Phosphate-induced release of arsenic from soils contaminated with lead arsenate. Soil Sci. Soc. Am. J. 55, 1301–1306.

Peryea, F.J., Kammereck, R., 1997. Phosphate-enhanced movement of arsenic out of lead arsenate-contaminated topsoil and through uncontaminated subsoil. Water Air Soil Poll. 93 (1–4), 243–254.

Pichler, T., Veizer, J., 1999. Precipitation of Fe III oxyhydroxide deposits from shallow-water hydrothermal fluids in Tutum Bay, Ambitle Island, Papua New Guinea. Chem. Geol. 162, 15–31.

Pichler, T., Veizer, J., Hall, G.E.M., 1999. The natural input of extremely high arsenic concentrations into a coral reef ecosystem by hydrothermal fluids and its removal by Fe(III) oxyhydroxides. Environ. Sci. Technol. 33, 1373–1378.

Pichler, T., Hendry, J., Hall, G.E.M., 2001. The mineralogy of arsenic in uranium mine tailings at the rabbit lake in-pit facility, Northern Saskatchewan, Canada. Environ. Geol. 40, 495–506.

Price, R.E., Pichler, T., 2006. Abundance and mineralogical association of arsenic in the Suwannee Limestone (Florida): implications for arsenic release during water-rock interaction. Chem. Geol. 228, 44–56.

Regnier, P., Lasaga, A.C., Berner, R.A., Han, O.H., Zilm, K.W., 1994. Mechanism of CO_3^{2-} substitution in carbonate flurapatite: Evidence from FTIR spectroscopy, ^{13}C NMR, and quantum mechanical calculations. Am. Mineral. 79, 809–818.

Scott, T.M., 1988. The lithostratigraphy of the Hawthorn Group (Miocene) of Florida. Florida Geol. Surv. Bull., 59.

Scott, T.M., 1990. The lithostratigraphy of the Hawthorn Group of peninsular Florida. Open File Report Florida Geol. Surv., 36.

Shaw, H.F., Wasserburg, G.J., 1985. Sm–Nd in marine carbonates and phosphates: implications for Nd isotopes in seawater and crustal ages. Geochim. Cosmochim. Acta 49, 503–518.

Shields, G., 2002. Phosphorites: a mine of information. Econ. Geol. Res. Unit Newslett, 6–7.

Skinner, H., Catherine, W., 2002. In praise of phosphates, or why vertebrates chose apatite to mineralize their skeletal elements. In: Ernst, W.G. (Ed.), Frontiers in Geochemistry; Organic, Solution, and Ore Deposit Geochemistry; Konrad Krauskopf, vol. 2. International Book Series, pp. 41–49.

Smedley, P.L., Kinniburgh, D.C., 2002. A review of the source, behavior and distribution of arsenic in natural waters. Appl. Geochem. 17, 517–568.

Stow, S.H., 1969. The occurrence of arsenic and the color-causing components in Florida land-pebble phosphate rock. Econ. Geol. 64, 667–671.

Swan, A.R.H., Sandilands, M., 1995. Introduction to Geological Data Analysis. Blackwell Science, Oxford.

Thomas, R.C., Saunders, J.A., 1998. Arsenic coprecipitation in low temperature pyrites: implications for bioremediation via sulfate reducing bacteria. Geol. Soc. Am. Abstr. Prog. 30 (7), A58.

Walsh, E., 2001. Arsenic drinking water standard issued: after seven-month scientific review, EPA backs Clinton-established levels. In: The Washington Post, p. A31.

Wang, Q., Morse, J.W., 1996. Pyrite formation under conditions approximating those in anoxic sediments: I. Pathway Morphol. Mar. Chem. 52, 99–121.

Wingard, G.L., Weedman, S.D., McCartan, L., 1993. Age and diagenesis of Miocene and Oligocene strata of the intermediate and upper Floridan Aquifer systems in Southwest Florida. Geol. Soc. Am. Abstr. Prog. 25 (6), 208.

Wright, J., 1990. Conodont apatite: structure and geochemistry. In: 28th Internat. Geol. Congr., Paleontological Society and American Geophysical Union, Washington, D.C., pp. 445–449.